Localized solutions for Plane Couette Flow: a continuation study

John Platt
Harvard University

1 Introduction

There has been much interest in investigating the transition to turbulence of linearly stable shear flows from a dynamical systems viewpoint [*Lanford*(1982), *Kerswell*(2005), *Eckhardt et al.*(2007)]. Here an instantaneous velocity field is pictured as a point in an infinite-dimensional phase space, with laminar flow being a linearly stable fixed point. Other invariant solutions exist, forming a "scaffold" for turbulent dynamics. Turbulence is imagined as a path in phase space moving between these invariant solutions. In this project we focus on one such invariant solution for plane Couette flow, in which the shear flow is established by moving two parallel plates past each other. A sketch of the geometry of the plane Couette system is shown in Figure 1.

The first of these invariant solutions was found by Nagata [*Nagata*(1990)], though many more have been found since [*Gibson et al.*(2009)]. Due to the vast computational expense required to work with these solutions, the majority of these solutions have been found in small domains that are periodic in both span-wise and stream-wise directions. However, observations of turbulent flows show localized turbulent regions coexisting with laminar regions [*Emmons*(1951), *Tillmark*(1992)]. A first invariant solution exhibiting this localized nature was presented in [*Schneider et al.*(2010a)], with the solution remaining periodic in stream-wise direction, but localized in the span-wise direction. In this project, building on the work outlined above, we try to provide more insight into these localized invariant solutions.

We aim to answer two main questions in this project. Our first goal is to determine what behavior should be expected for localized invariant solutions of plane Couette flow. To investigate this we first review the observations from for the first localized solution

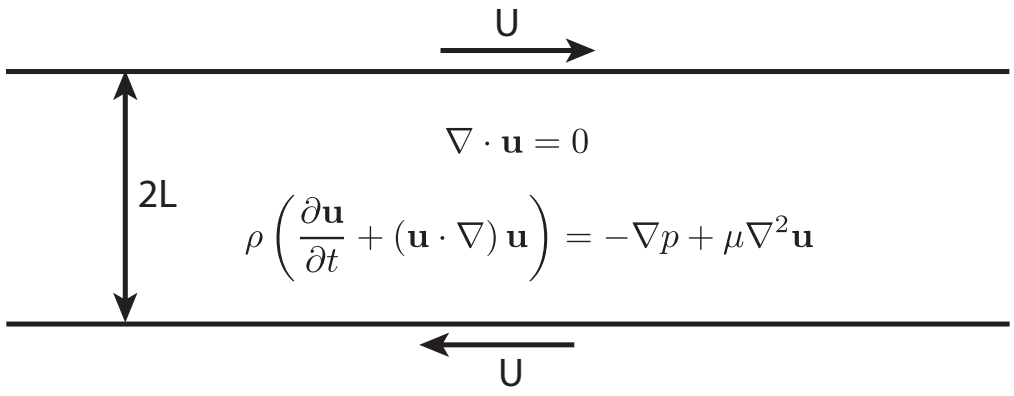

Figure 1: A sketch of the plane Couette system. Two plates separated by a distance of $2L$ are moved past each other with a velocity difference of $2U$, establishing a shear flow in the viscous fluid between the plates.

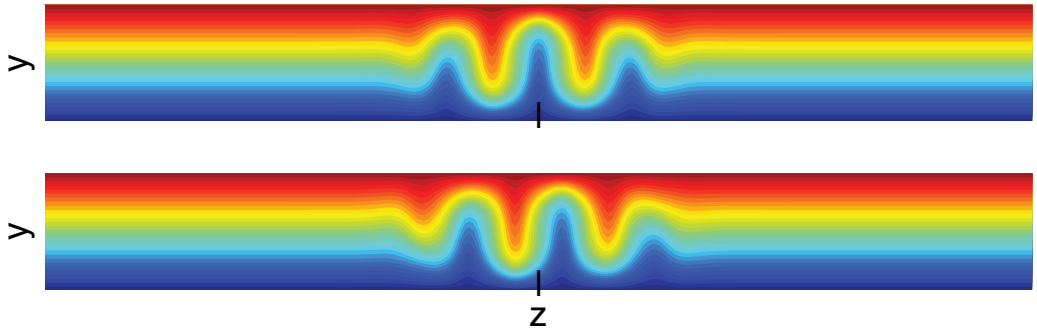

Figure 2: Plots of x-averaged streamwise velocity for the two localized solutions presented in [*Schneider et al.*(2010b)].

[*Schneider et al.*(2010b)], which show a distinctive bifurcation behavior known as homoclinic snaking. We then use continuation methods to investigate the bifurcation structure of the second solution, and compare the two solutions to see what similarities and differences they share. The second goal is to investigate how more localized solutions could be generated. We analyze the symmetry breaking process during localization, and predict the number of localized "versions" of a periodic solution that may exist. All of the numerical calculations in this project are performed using the Channelflow package developed by John Gibson, and approximately 25,000 hours of CPU time was used to produce the results.

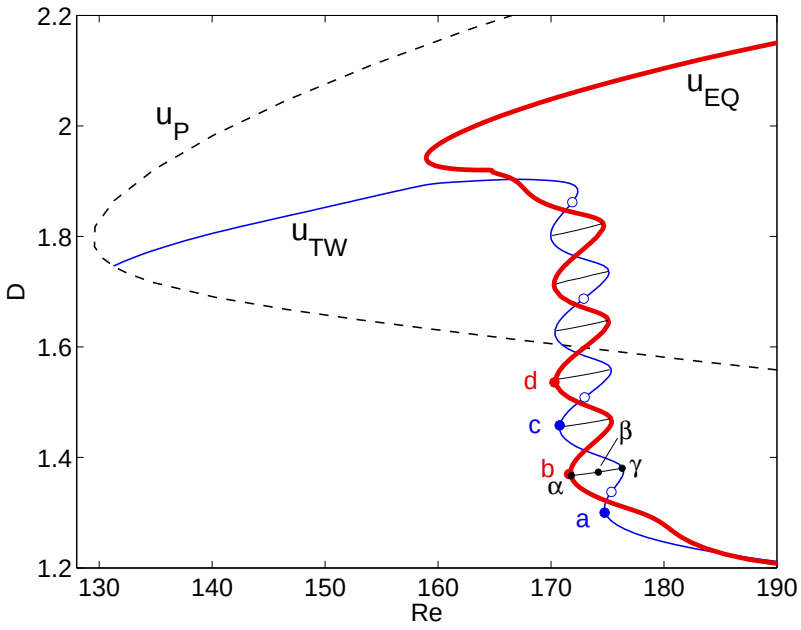

Figure 3: A plot of the bifurcation diagram from [*Schneider et al.*(2010b)]. We clearly see the homoclinic snaking structure, and the reattachment to the periodic solution from [*Nagata*(1990)].

2 Review of the first localized solution

[*Schneider et al.*(2010b)] presented a continuation study for the first localized solution ever found for plane Couette flow. The periodic counterpart for this localized solution is the original invariant solution presented in [*Nagata*(1990)], and there exist two distinct versions of the solution, with flowfields shown in Figure 2. Continuing the pair of solutions in Re, for a fixed value of the x-dimension of the periodic domain, L_x, produced the bifurcation diagram shown in Figure 3. Here D is a volume normalized dissipation rate, and can be thought of as a measure of how turbulent the solution is. The two solutions intertwine in a sequence of saddle-node bifurcations to form a structure that transitions to higher values of D over a relatively short interval in Re. One of the solutions reattaches to the periodic solution, shown in black, while the other solution follows the upper branch to high Re.

This sort of structure has also been observed in an entirely different system, the Swift-Hohenberg equation,

$$\frac{\partial u}{\partial t} = ru - \left(\frac{\partial^2}{\partial x^2} + q_c^2\right)^2 u + f(u), \tag{1}$$

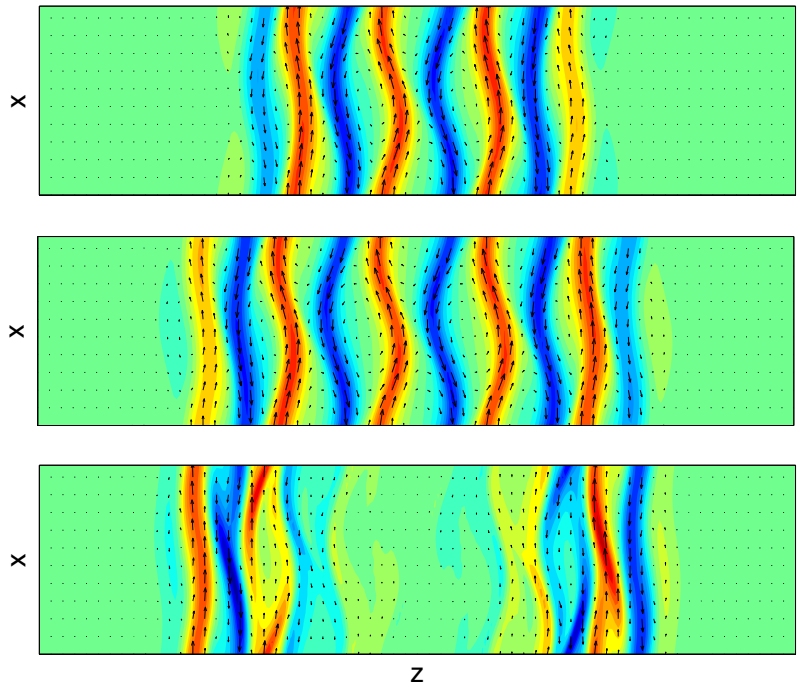

Figure 4: Plots showing the velocity field on the midplane. In-plane velocities are indicated with arrows and streamwise velocity is indicated with color. The top pair of plots show the flowfield at two adjacent saddle-node bifurcations on the snake, and the bottom plot show the marginal eigenfunction at the upper bifurcation.

where r is the control parameter, q_c is a parameter, and $f(u)$ is a nonlinear function. The phenomena is known as homoclinic snaking [*Burke and Knobloch*(2007)], and describes how a spatially localized solution of the above equation expands to fill the periodic domain it sits in. As the solution grows, structure is added at the edges, while in the internal region the solution does not change. Thus, to further test the similarities between the results in [*Schneider et al.*(2010b)] and homoclinic snaking in the Swift-Hohenberg equation, we can examine the flow fields at different points on the snake. Throughout this project we take $\mathbf{x} = (x, y, z)$ with y being the direction perpendicular to the plates, x parallel to the direction of shear, and z the spanwise coordinate. These coordinate directions are then used to define the velocity vector $\mathbf{u} = (u, v, w)$. Figure 4 shows flowfields on the midplane for the

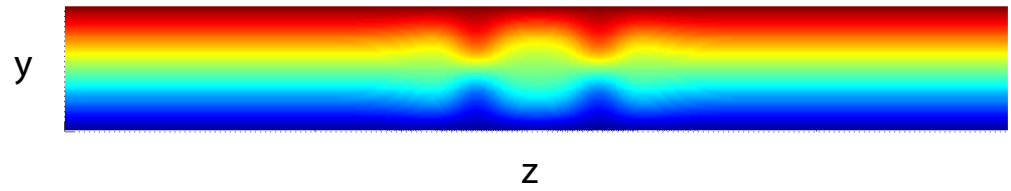

Figure 5: A plot of x-averaged streamwise velocity for the new localized solution.

first two saddle node bifurcations in Figure 3, along with the marginal eigenfunction for the second bifurcation. From the marginal eigenfunction we can clearly see that the solution is adding structure at the edges of the localized solution, while the central part remains relatively unchanged. As we move up the snake the solution achieves higher values of D by expanding the non-laminar region, but keeping the magnitude of the local dissipation rate roughly constant.

In the next section we present the results of a continuation study on a second localized solution. We want to compare the observations of this second solution with the results summarized above, to allow us to see what behavior is generic for localized invariant solutions, and specifically if homoclinic snaking is a feature of all localized solutions of plane Couette flow.

3 Continuation of second solution

We now use continuation methods to investigate a second localized solution. This localized solution was found by [*Gibson and Brand*(2011)] based on an understanding of the functional form of the fronts between laminar and turbulent regions. It is a localized version of the periodic solution EQ7 from [*Gibson et al.*(2009)]. Figure 5 shows a plot of the x-averaged streamwise velocity, allowing us to directly compare with the previous localized solution shown in Figure 2. We notice that the variations in velocity for the new localized solution are less pronounced, in agreement with the observation that this new solution exists at a much lower dissipation.

To allow us to plot the bifurcation diagrams, in the following we describe flowfields by

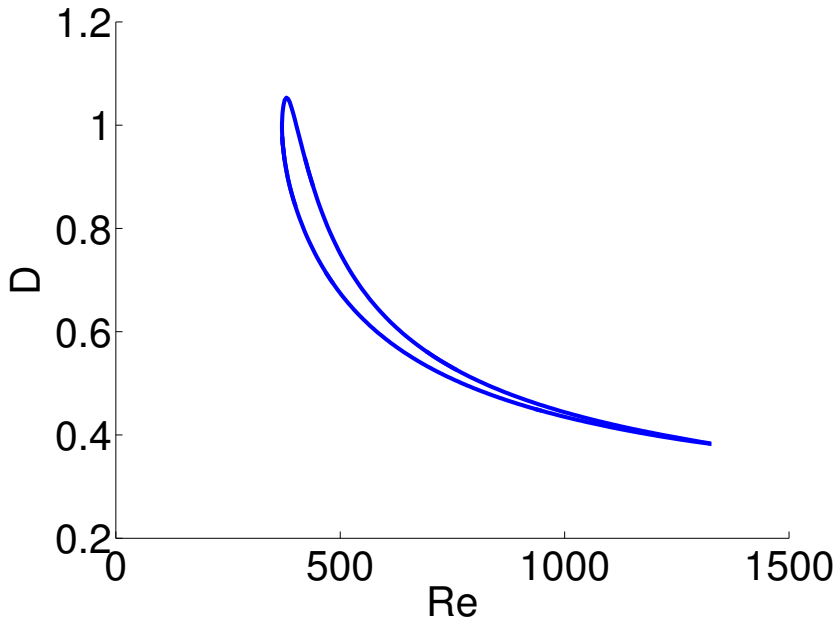

Figure 6: A plot of the bifurcation diagram generated by continuing in Re with $L_x = 3\pi$.

the simple measure,

$$D = \frac{1}{2L_x}\int_{-L_z/2}^{L_z/2}\int_{-1}^{1}\int_{-L_x/2}^{L_x/2}\mathbf{v}(\mathbf{x})\mathrm{d}x\mathrm{d}y\mathrm{d}z, \tag{2}$$

where $\mathbf{v}$ is the velocity perturbation found by subtracting the laminar profile away from the full velocity field, and L_x, L_z are the streamwise and spanwise dimensions of the periodic domain. We do not normalize by L_z since our solutions are localized in L_z, and thus any measure of them should also be independent of L_z. Since the solution is independent of L_z, we have just two controlling parameters Re and L_x to continue in.

3.1 Isolas

To begin we continue in Re, fixing $L_x = 3\pi$, producing the results shown in Figure 6. We observe a closed isola in the (Re, D) plane, in sharp contrast to the homoclinic snaking observed with the first localized solution. We also note that the solution is relatively constant over a wide range of Re. Such closed isolas have also been observed in studies of localized solutions in the Swift-Hohenberg equation [*Burke and Knobloch*(2006)]. Recalling that for the previous localized solution higher values of D were attained by approximately

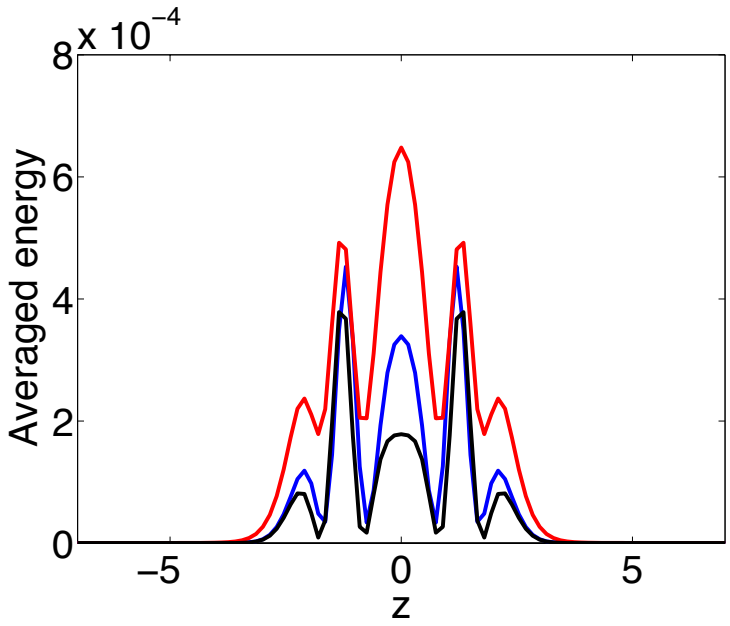

Figure 7: A plot of the averaged energy as a function of z for three points on the $L_x = 3\pi$ isola. The solution with the lowest value of Re is plotted in red, the highest value of Re in black, and the intermediate value of Re in blue.

fixing the maximum size of the velocity perturbations, but expanding the solution to fill more of the domain, we now plot the energy in the velocity fluctuations, averaged in the x and y-directions, as a function of z at three points on the closed curve; the two extreme values of Re and one intermediate value. This is shown in Figure 7. We see that the structure of the solutions remains relatively constant, while changes in D are achieved by varying the amount of energy in each of the oscillations. This is in agreement with the observations of isolas in the Swift-Hohenberg equation in [*Burke and Knobloch*(2006)], which show that around an isola the number of oscillations in the solution is unchanged. We can also compute the spectrum of the solution at a selection of points, finding that at all points the solution has a low number of unstable directions. This is important for the dynamical systems view of turbulence since points in phase space with few unstable directions may be approached more often than ones with many unstable directions.

Next we continue the original localized solution in L_x, producing the results in Figure 8. This time we do not observe a closed curve, instead seeing a relatively constant value of D

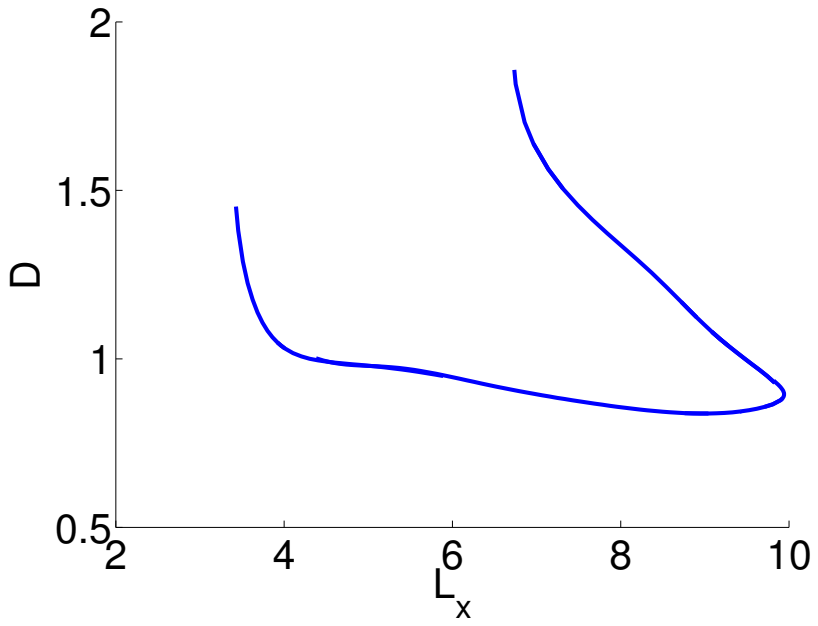

Figure 8: A plot of the bifurcation diagram generated by continuing in L_x with $Re = 400$.

over a range of L_x with the two ends of the curve moving towards higher values of D. Our previous continuation in Re with $L_x = 3\pi$ had two values at $Re = 400$, corresponding to the two points on the curve for $L_x = 3\pi$. As before, when we examine the flowfields along the curve in Figure 8 we see relatively little change in the structure, with higher values of D be attained by increasing the magnitude of the velocity fluctuations not increasing the fraction of the domain the localized solution occupies.

Now we use the solutions found at different values of L_x to begin new continuations in Re, shown in Figure 9. For $L_x = 2.9\pi, 3\pi, 3.1\pi$ we see very similar behavior to before. However, for $L_x < 2.9\pi$ we see a region of higher curvature developing for low values of Re. For these values of L_x we take the second solution at $Re = 400$, which exists at a higher value of D, and continue in L_x. We discover that the reason for the change in behavior around $L_x = 2.9\pi$ is due to the existence of another solution branch, shown in red in Figure 10. Continuing the new curve in one direction leads to a roughly constant value of D extending to far higher values of L_x than previously observed. Extending the curve in the other direction we see some curves before the solution branch rapidly moves to higher

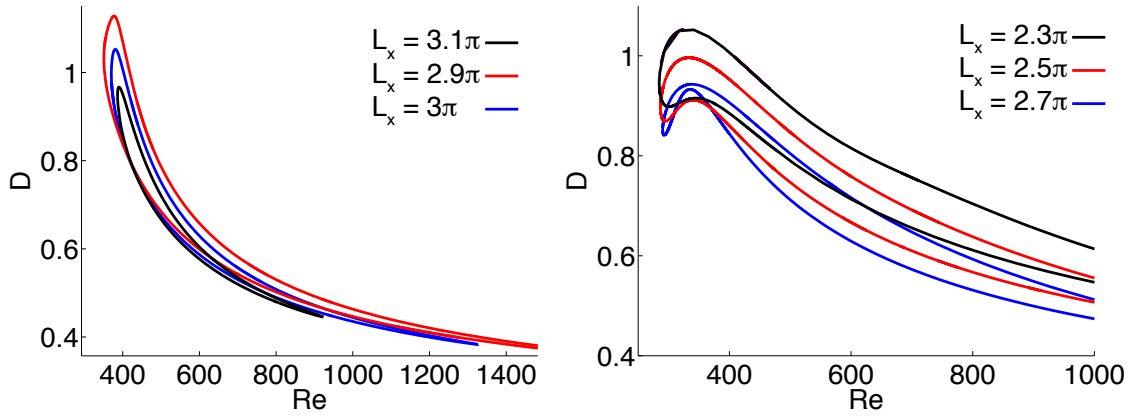

Figure 9: A plot of the bifurcation diagrams generated by continuing in Re for a range of L_x values.

values of D.

3.2 Searching for snaking

So far we have seen no evidence of homoclinic snaking, but the existence of the new curve for $L_x \in [2.9\pi, 3.1\pi]$ demonstrates the existence of further curves in the (Re, D) plane, to go with the isolas already observed. Choosing $L_x = 2.9\pi$ we track this new curve, shown in red in Figure 11. We observe dramatically different results, with the new curve showing snaking like behavior and moving to much higher values of D in a relatively narrow range of Re. Similar results are seen when continuing solutions from the new branch in the (L_x, D) plane in Re. Fixing $L_x = 4\pi$ and continuing in Re we produce the results seen in Figure 12. As in Figure 11 the curve proceeds to high values of D in a narrow range of Re, exhibiting some bends. To test if this could be another instance of homoclinic snaking we examine the flow fields. Figure 13 shows the averaged energy as a function of z for three points along the $L_x = 4\pi$ curve. We observe that, while there is some evidence of additional structure being added at the edge of the localized solution, as before the higher values of D are achieved by increasing the magnitude of the velocity fluctuations. A similar investigation of the flowfields along the $L_x = 2.9\pi$ curve gives the same result.

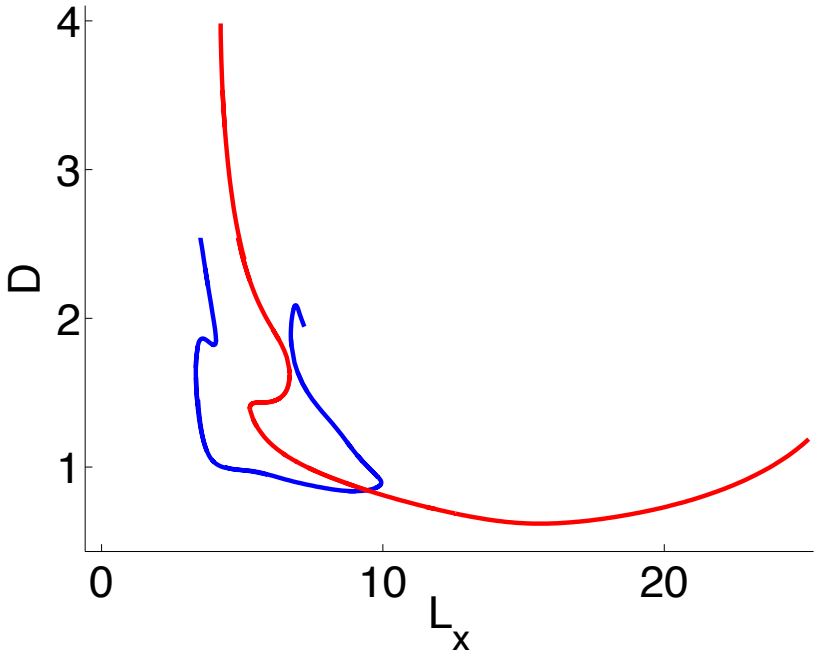

Figure 10: A plot of the bifurcation structure in the (L_x, D) plane, for $Re = 400$, with the new branch included.

3.3 Bifurcation behavior summary

To summarize we have found that homoclinic snaking is not a feature of all localized solutions of plane Couette flow. The bifurcation behavior shown by our localized solutions very different to that observed in [*Schneider et al.*(2010b)]. For some continuations in Re we see closed curves, as in some continuation studies of the Swift-Hohenberg equation [*Burke and Knobloch*(2006)]. The physical properties of the solutions also vary considerably. When compared with the first localized solution, our localized solution exists at much lower dissipation values, and remains there for a wide range of Re and L_x. Our solutions also retains the property of having a relatively low number of unstable directions, and important property for the dynamical systems view of turbulence. Several branches at higher values of D are still open for further continuation, and these may provide a route to the values of D seen with the previous solution. Having discussed the bifurcation behavior for localized solutions, we next discuss further work aimed at finding additional localized

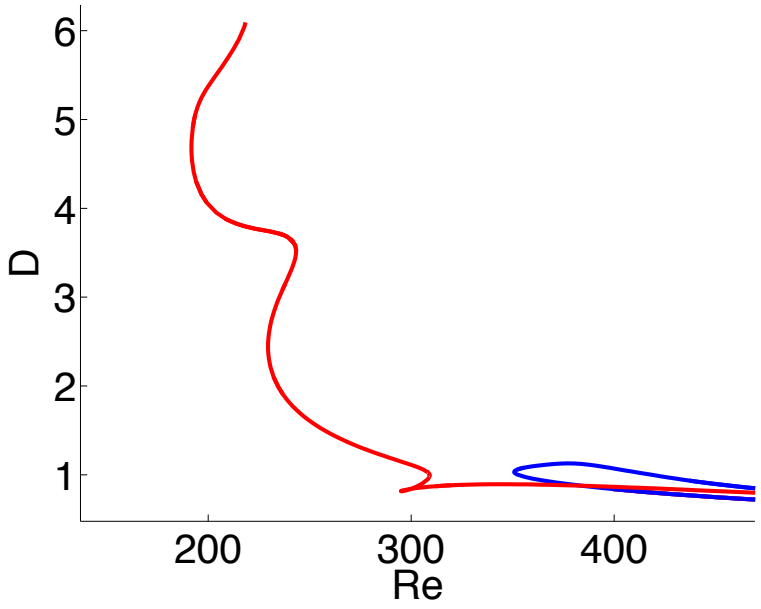

Figure 11: A plot of the (Re, D) bifurcation diagram for $L_x = 2.9\pi$, showing the two distinct branches.

solutions.

4 Symmetry breaking during localization

The localized solution discussed in this project is just the second one discovered, despite the existence of many solutions in spanwise periodic domains. We will now address our second goal of investigating how additional localized solutions could be generated. New work examining the fronts between laminar and turbulent regions has shown how more localized solutions could be constructed using the many periodic solutions currently known [*Gibson and Brand*(2011)]. We now examine the symmetries of both localized solutions, and try to find general relations between these and the symmetry groups of the periodic parent solutions. We hope that this will provide useful guidance when attempting to find future localized solutions, and we also make a prediction for the number of localized versions of each periodic solution.

First we define the symmetry groups for the exact solutions using the notation in

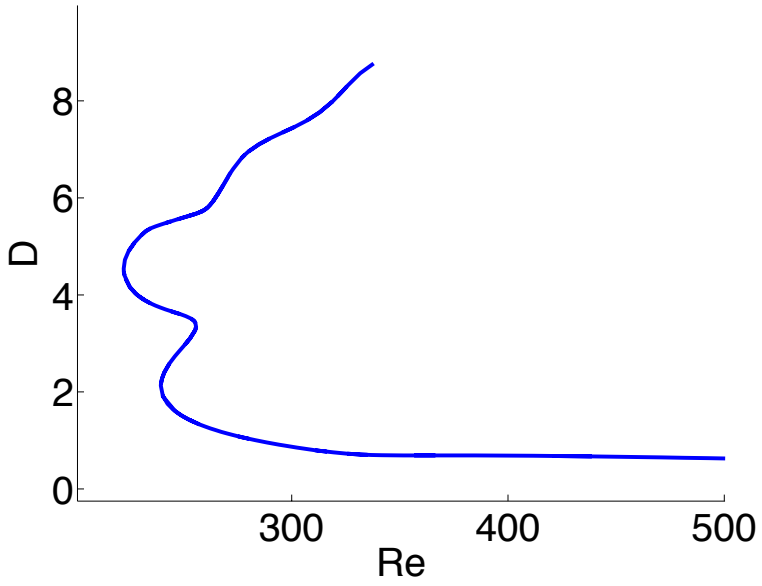

Figure 12: Bifurcation diagram generated by continuing in Re with $L_x = 4\pi$.

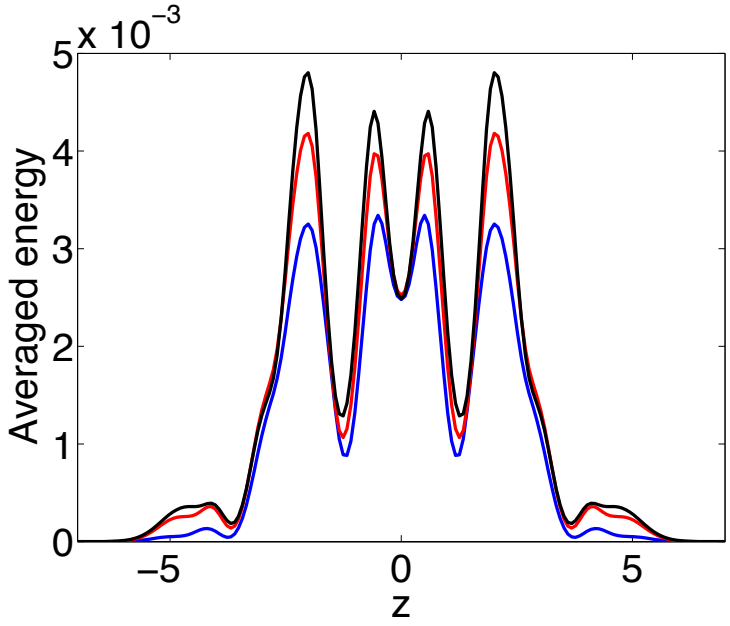

Figure 13: A plot of the averaged energy as a function of z for three points on the $L_x = 4\pi$ curve.

[*Gibson et al.*(2009)]. Plane Couette flow in a periodic box allows symmetries of the form

$$[u, v, w](x, y, z) = [s_x u, s_y v, s_z w](s_x x + \tau_x L_x, s_y y, s_z z + \tau_z L_z). \tag{3}$$

Here s_x, s_y and s_z define the reflection symmetries in x, y and z respectively, with τ_x and τ_z setting the shift in the x and z directions. An individual symmetry can then be fully described using the notation

$$(1, s_x, s_y, s_x; \tau_x, \tau_z).$$

Obviously solutions can satisfy multiple symmetries, which themselves can be combined to form a symmetry group for the solution. We can analyze the symmetries of solutions by investigating the generators of the symmetry groups.

First we examine the localized solution presented in [*Schneider et al.*(2010a)], which is a localized version of the first periodic solution found in [*Nagata*(1990)]. The symmetry group for the periodic solution has two generators,

$$(1, 1, 1, -1; 0.5, 0)$$

$$(1, -1, -1, -1; 0, 0.5)$$

This led to two localized solutions, one a strict equilibrium, the other a travelling wave. Each of these solutions has a symmetry group with a single generator,

$$(1, 1, 1, -1; 0.5, 0)$$

for the travelling wave, and,

$$(1, -1, -1, -1; 0, 0)$$

for the equilibrium.

Next we turn to the localized solution studied in this work. In this case the periodic parent has a symmetry group with three generators,

$$(1, -1, -1, 1; 0, 0)$$

$$(1, 1, 1, -1; 0, 0.5)$$

$$(1, 1, 1, -1; 0.5, 0)$$

This leads to a localized solution that has a symmetry group with just two generators,

$$(1, -1, -1, 1; 0, 0)$$

$$(1, 1, 1, -1; 0, 0)$$

From this limited set of examples we now extrapolate some general rules. The localization process breaks one of the symmetry generators of the periodic parent solution, leading to a symmetry group with one fewer generator. Any shift in the L_z direction is eliminated. In [*Schneider et al.*(2010a)] two solutions were found, corresponding to breaking each of the generators of the Nagata solution in turn. For the new solution discussed here we have broken a single generator, allowing us to tentatively predict the existence of two more localized versions of the periodic solution, corresponding to breaking the other two periodic generators. Even more speculatively we can predict the existence of three more, giving six in total, if localized solutions can be formed from any subgroup of the periodic symmetry group.

5 Discussion

In this project we analyzed the physical flowfields and bifurcation structure for a localized exact solution for plane Couette flow. By making comparisons with the first such solution we can begin to determine what behavior is generic for localized solutions of plane Couette flow, and what is specific to individual solutions.

The previous localized solution showed a distinctive bifurcation behavior, identical in form to the homoclinic snaking seen in the Swift-Hohenberg equation. Despite an extensive parameter search we can find no evidence for homoclinic snaking in this solution, suggesting that this bifurcation structure is not an essential feature of all localized solutions. However, we did find closed curves in the bifurcation diagram, similar to the isolas observed in some studies of the Swift-Hohenberg equation. In contrast to the previous study, for which solutions existed in a narrow range of Re, we found relatively unchanged solutions over a wide range of Re and L_x. The solutions presented in this study also exist at far lower dissipation values than previous observations.

To conclude, localized solutions for plane Couette flow can experience a wider range of behavior than that reported in [*Schneider et al.*(2010b)]. Solutions can exist over a wider range of Re, L_x and D then previously observed, and do not necessarily show the distinctive homoclinic snaking bifurcation behavior. However, there may still be a link to the Swift-Hohenberg equation, as shown by the isolas observed in this study.

References

[*Kerswell*(2005)] Kerswell, R.R. (2005), Recent progress in understanding the transition to turbulence in a pipe, *Nonlinearity*, 18.

[*Eckhardt et al.*(2007)] Eckhardt, B., T.M. Schneider, B. Hof, and J. Westerweel (2007), Turbulence transition in pipe flow, *Annual Review of Fluid Mechanics*, 39.

[*Lanford*(1982)] Lanford, O.E. (1982), The strange attractor theory of turbulence, *Annual Review of Fluid Mechanics*, 14.

[*Nagata*(1990)] Nagata, M. (1990), Three-dimensional finite-amplitude solutions in plane Couette flow: bifurcation from infinity, *Journal of Fluid Mechanics*, 217.

[*Waleffe*(2003)] Waleffe, F. (2003), Homotopy of exact coherent structures in plance shear flows, *Physics of Fluids*, 15.

[*Gibson et al.*(2009)] Gibson, J.F., J. Halcrow, and P. Cvitanovic (2009), Equilibrium and travelling-wave solutions of plane Couette flow, *Journal of Fluid Mechanics*, 638.

[*Tillmark*(1992)] Tillmark, N., and P.H. Alfredsson (1992), Experiments on transition in plane Couette flow, *Journal of Fluid Mechancis*, 235.

[*Emmons*(1951)] Emmons, H.W. (1951), The laminar-turbulent transition in a bounary layer - Part I, *Journal of the Aeronautical Sciences*, 18.

[*Schneider et al.*(2010a)] Schneider, T.M., D. Marinc, and B. Eckhardt (2010), Localized edge states nucleate turbulence in extended plane Couette cells, *Journal of Fluid Mechanics*, 646.

[*Schneider et al.*(2010b)] Schneider, T.M., J.F. Gibson, and J. Burke (2010), Snakes and ladders: Localized solutions of plane Couette flow, *Physical Review Letters*, 105.

[*Burke and Knobloch*(2007)] Burke, J., and E. Knobloch (2007), Homoclinic snaking: Structure and stability, *Chaos*, 17.

[*Burke and Knobloch*(2006)] Burke, J., and E. Knobloch (2006), Localized states in the generalized Swift-Hohenberg equation, *Physical Review E*, 73.

[*Gibson and Brand*(2011)] Gibson, J., and E. Brand (2011), Spatially localized solutions of plane Couette flow, *64th Annual Meeting of APS Division of Fluid Dynamics*, 56.